2024

Methodology, deployment, and performance of pico balloons in Antarctica

Todd McKinney

METHODOLOGY, DEPLOYMENT, AND PERFORMANCE OF PICO BALLOONS IN ANTARCTICA

Todd McKinney

A THESIS

Submitted in partial fulfillment of the requirements
for the degree of Master of Science
in
The Department of Atmospheric and Earth Science
to
The Graduate School
of
The University of Alabama in Huntsville

May 2024

Approved by:

Dr. Mike Newchurch, Research Advisor/Committee Chair
Dr. Udaysankar Nair, Committee Member
Dr. Sundar Christopher, Committee Member
Dr. Lawrence Carey, Department Chair
Dr. Rainer Steinwandt, College Dean
Dr. Jon Hakkila, Graduate Dean

Abstract

During the 2022/2023 Antarctic summer, eight pico balloon flights from Neumayer Station III unveiled insights into Antarctic troposphere/stratospheric winds (9 - 15 km AMSL). The most impressive flight lasted an astounding 98 days, completing eight circumnavigations of the Southern Hemisphere. Flight data indicated zonal velocities from -50 to 250 km hr^{-1} and meridional velocities of $\pm$100 km hr^{-1}, with total wind speeds from 2.0 to 270 km hr^{-1}. Pico balloons can ascend due to convection, altering their float density. They also drift further south than larger stratospheric balloons, reaching latitudes close to the south pole. This study showcases the transformation of budget-friendly party balloons into effective research tools, emphasizing their logistical simplicity: all materials except lifting gas were transported to Antarctica in one person's carry-on. The work promotes pico balloons' wider scientific application.

Acknowledgements

This work was adapted from publication https://doi.org/10.1175/JTECH-D-23-0047.1. Many thanks to the University of Alabama in Huntsville College of Science, the Atmospheric and Earth Science department, and the Earth System Science Center for funding. I express my sincere gratitude to Neumayer-Station III for their gracious hospitality. Thanks go out to Markus Schulze for providing invaluable assistance with balloon launches and logistics. In addition, I extend my appreciation to Tom Medilin and the W5KUB group, Jim Janiak with the Northern Illinois Bottlecap Balloon Brigade, and Michael Seedman for their contributions towards balloon trackers. Lastly, I thank Dr. Mike Newchurch and my thesis committee for their mentorship.

Table of Contents

List of Figures

List of Tables

List of Variables

- P_b - burst pressure (Pa)
- F_{B} - force due to buoyancy (kg m s^{-2})
- F_g - force due to gravity (kg m s^{-2})
- V_g - volume of gas at the surface (m^3)
- V_f - balloon volume when fully inflated (m^3)
- R_d - gas constant for dry air, 287.053 J K^{-1} kg^{-1}
- ρ_a - density of air at sea level at 0°C, 1.225 kg m^{-3}
- ρ_g - density of lifting gas at sea level at 0°C, Helium: 0.1785 kg m^{-3}, Hydrogen: 0.0899 kg m^{-3}
- m_b - mass of the balloon (kg)
- m_p - mass of the payload (kg)
- m_g - mass of the lifting gas (kg)
- ρ_{float} - balloon float density (kg m s^{-3})
- F_L - free lift (kg)
- N_L - neck lift (kg)
- C_D - drag coefficient
- A - cross-sectional area (m^2)
- V - vertical velocity (m^2
- ΔP - differential pressure (Pa)
- P_{float} - Pressure at float altitude (Pa)
- $T_{surface}$ - Temperature at surface (K)
- ρ_{float} - kgm^{-3}

- T_{float} - Temperature at float altitude (K)
- m_{bs} (kg)

  Note: while all computations are performed using base metric units (Pa for pressure, kg for mass, K for temperature), we express balloon pressures in psi and masses in g. This adjustment caters to the typically small values encountered in pico ballooning, making these units more practical for measurements.

Chapter 1. Introduction

Super-pressure balloons (SPBs) are specialized high-altitude balloons designed to maintain a constant float altitude over a long period of time. SPBs have demonstrated their effectiveness in conducting atmospheric studies in Antarctica, a region that presents a unique and challenging environment for scientific research due to its weather conditions and remote location. Previous Antarctic SPB campaigns, such as the Vorcore campaign [14], the THORPEX campaign [7], the Loon project [10], the Concordiasi project [22], and various National Aeronautics and Space (NASA) campaigns [16, 6], have successfully flown balloons at float altitudes between 20 km and 40 km AMSL. These balloons have diameters ranging between 15-30 m and can support payloads up to 3600 kg. The logistical and safety demands for these SPB flights are significant due to their large size and heavy payloads. For example, during the Vorcore campaign, weather restrictions limited launch opportunities, with only 66-percent of the campaign days suitable for a safe launch; strong surface winds and gusts exceeding 14 km hr^{-1} and 22 km hr^{-1}, respectively, made launches of these larger balloons impossible. In addition, out of the 27 Vorcore balloons deployed, 9 flights were terminated due to flight restrictions that required grounding the balloons to prevent crossing the

Figure 1.1: Micro super pressure balloon tethered shortly before launch. Transmitter is below the hands of the person launching. Neumayer station is in the background.

40.0°S latitude line or flying below the 100 hPa pressure level. These restrictions highlight the operational limitations of larger SPBs.

Pico balloons, also known as micro super pressure balloons, are smaller than typical SPBs, with diameters ranging from 0.5-2 m and a payload capacity of less than 50 g. The smaller size of pico balloons enables them to be deployed in greater numbers and in a more diverse range of locations compared to large SPBs. Additionally, the reduced size of pico balloons results in lower launch and labor costs, where each launch can be conducted by a single person. For example, a regular weather balloon released at a weather balloon facility requires approximately 1.70 m^3 of helium, whereas launching a single pico balloon only requires

about 0.07 m^3 of helium. Consequently, one could conduct 24 pico launches using the same amount of helium needed for a single weather balloon launch. Figure 1.1 shows a balloon just before launch.

Before the advancement of low-weight radio and satellite-telemetry systems, smaller Mylar super pressure balloons served as reflectors, often to calibrate radars [3]. With the development of smaller, low-cost amateur-radio technology, hobbyists now often deploy and track pico balloons for fun [4]. In addition, using a certain pressure-testing process (first documented in this paper), anyone can turn a normal party balloon into a pico balloon. Only recently have pico balloons served as a scientific resource; [18] conducted three pico balloon flights from the northern hemisphere in early 2021, demonstrating their effectiveness for atmospheric trajectory studies. Pico balloons provide a unique perspective on the interactions between the troposphere and stratosphere due to their lower float altitudes. Because of the size and payload weight, pico balloons can travel to a wide variety of locations while still following globally recognized Federal Aviation Administration's PART 101 regulations [9].

This study describes the launch of and data collected from eight pico balloons deployed from Antarctica during the 2022/23 summer season deployed from Neumayer-Station III (70.6666° S, 8.2667° W) [32] in November 2022. Table 1.1 shows a summary of the fights. We first provide information on the payloads used and the mathematical background and principles underlying the use of pico balloons. Then, we describe a pressure testing method we developed in order to

improve odds of a successful launch and flight. Finally, data from the balloon flights is presented and discussed.

Table 1.1: Flight information of the balloons launched in this study. *Represents the balloon that had restricted telemetry capabilities, indicating that its transmissions could only be received within the line of sight of Neumayer Station III. As a result, the date range, flight duration, circumnavigations, and latitude range remain uncertain. † Represents the balloon that had a leak shortly after launch.

Balloon Callsign	**Date Range**	**Flight Duration(day)**	**Circum-navigations**	**Latitude Range**
*K4UAH-3	13 November 2022 — 17 January 2023	64	1	70.649°S —73.221°S
K4UAH-1	16 November 2022 — 14 January 2023	58	5	87.312°S —43.229°S
W5KUB-114	16 November 2022 — 17 January 2023	61	5	78.438°S — 6.175°S
K4UAH-2	20 November 2022 — 29 December 2022	39	3	86.646°S —21.938°S
K4UAH-4	20 November 2022 — 12 February 2023	84	7	85.396°S —22.104°S
K4UAH-6	20 November 2022 — 6 February 2023	78	6	88.479°S —38.688°S
W5KUB-115	23 November 2022 — 3 March 2023	97	8	88.770°S —13.313°S
†K4UAH-5	29 November 2022	<1	0	70.729°S —69.895°S

Chapter 2. Finding the Optimal Pico Balloon

2.1 Types of Pico Balloons

Pico balloons are made from durable materials such as polyethylene or mylar, which allow them to withstand pressure variations and maintain a consistent volume. Unlike latex, which is commonly found in party balloons and weather balloons, these materials are suitable for SPBs as they can effectively withstand the pressure differential between the interior and exterior of the balloon. When choosing a material for the manufacture of pico balloons, mass limitations must be considered. Mylar is generally heavier, resulting in smaller balloons that float at a lower altitude, while polyethylene balloons are lighter and can be made into larger volumes, allowing them to float at a higher altitude. Depending on the mission, a specific material and size can be selected to optimize altitude. For example, to float in the upper troposphere (9 km), a 0.76 m diameter mylar balloon could be used, while a lighter and larger 0.81 m diameter polyethylene balloon could float in the lower stratosphere (13 km). Additionally, different gases, such as helium or hydrogen, can be used to achieve different floating altitudes, with helium causing balloons to float lower and hydrogen causing them to float higher. The advantage of floating at higher altitudes is a decreased chance of encountering moisture, convection, or strong updrafts, which are the most common reasons

for pico balloon failure. In this study, helium was used because of its availability at Neumayer Station III.

In acquiring a pico balloon, there are two options: constructing one or purchasing one. This study focuses on utilizing commercially available polyethylene party balloons purchased from a party supply store [34].This study does not explore the construction process of pico balloons; rather, its main focus lies in evaluating the pressure resistance of easily accessible party balloons. For detailed information on building super pressure balloons, the authors refer readers to other relevant publications [25, 15, 33, 3]. For the balloons deployed in this paper, despite being marketed as 0.81 m diameter polyethylene balloons, our measurements revealed that the balloons actually had a diameter of approximately 0.74 m. This results in a volume of 0.20 m^3 when inflated. To assess the potential of a balloon platform as a pico balloons, there are three distinct phases of evaluation: pressure testing, float equations, and assessment of success criteria.

2.2 Pico Balloon Equations

The main forces to consider on the balloon are buoyancy, F_b, gravity, F_g, and aerodynamic drag, F_{D}, shown by the following equation:

$$F_{\mathrm{total}} = F_{\mathrm{B}} + F_g - F_{\mathrm{D}} = V_g \rho_{\mathrm{a}} g - (V_g \rho_{\mathrm{g}} + m_{\mathrm{b}} + m_{\mathrm{p}})g - \frac{1}{2} C_{\mathrm{D}} \rho_{\mathrm{a}} A V^2, \qquad (2.1)$$

where C_{D} is the drag coefficient, A is the cross-sectional area of the balloon, and V is the balloon velocity.

In ballooning, a quantity called free lift F_L is defined which has units of mass.

$$F_L = V_g \cdot [\rho_a - \rho_g] - (m_b + m_p). \tag{2.2}$$

Lift can easily be measured by measuring the tension in a tether and is proportional to the initial acceleration of the balloon. We can also find the mass of the lifting gas m_g, with

$$V_g \cdot \rho_g = m_g. \tag{2.3}$$

During the ascent the volume of the gas, V_g, increases while ρ_a decreases. We call the volume of the balloon when it is fully inflated V_f. Note that V_f and V_g are equal. We see that the air density at the float altitude is given by

$$\rho_{\mathrm{float}} = \frac{1}{V_f}(m_g + m_b + m_p). \tag{2.4}$$

and the float pressure is then

$$P_{\mathrm{float}} = \rho_{\mathrm{float}} R_d T. \tag{2.5}$$

And finally, we find the internal balloon pressure as

$$\Delta P = \frac{P_{\text{surface}} \cdot V_{\text{gas}} \cdot T_{\text{float}}}{T_{\text{surface}} \cdot \frac{m_{\text{bs}}}{\rho_{\text{float}}}}. \tag{2.6}$$

ΔP must be less than the burst pressure and greater than 0. A safe range is determined from the pressure testing protocol as shown in Figure 2.2 (discussed next section).

Note that V_f is ideally an intrinsic property of the balloon. As internal balloon pressure is increased (or external pressure on the balloon is decreased), the volume will increase until it reaches V_f. If the pressure differential is increased further, the balloon walls exert a force equal to the pressure differential to keep the balloon at V_f. If the pressure differential becomes higher than the balloon material is designed for, it will burst or in some cases become overstretched, causing V_f to increase. This can easily occur when the balloon is overfilled. If V_f were to remain constant, then adding more lifting gas than strictly necessary to the balloon would only cause the total balloon system mass to increase and result in a lower float altitude. However, in practice, we observe that pico balloons often fly higher when filled with more lifting gas. This is because higher F_L values provide faster ascent rates at launch. If a pico balloon rises too quickly, it will overshoot its estimated float density by enough that the increased differential pressure will cause the balloon to stretch, increasing V_f and thus the float altitude. These overstretched balloons are prone to leaking or bursting. A pressure testing protocol as described in the next section can be used to determine a "safe" free lift value for a certain type of balloon; typical free values are listed in Table 2.1 for pico balloons. Understanding how balloon volume changes during the transition

Table 2.1: Free lift values for pico balloons and their safety rating. A higher F_L can be obtained either by decreasing the mass of the payload or by increasing the volume of the gas at surface. If payload is decreased, the float altitude will be higher.

Free Lift Range (g)	Safety Rating	Description
$1 < F_L < 5$	Unsafe	A free lift in this range is often too low for constant float density as the balloon membrane is not fully pressurized when it achieves float.
$5 < F_L < 6$	Risky	This range offers a lower chance of burst, but is still considered low.
$6 < F_L < 7$	Safe	A good balance between safety and float altitude.
$7 < F_L < 8$	Moderate	Higher float altitude with increased resistance against ice buildup on the balloon. Higher burst risk during ascent.
$8 < F_L < 10$	Risky	Much higher float altitude and extreme resistance against ice buildup. Significantly higher burst risk during ascent.
$10 < F_L$	Unsafe	Often too high for stable float; rapid ascent can cause bursting.

from ascent to float is one of the main challenges of working with pico balloons. Because pico balloons are often cheap and not quality controlled, it is sometimes difficult to quantify how the material behaves at higher altitudes.

Now that the base equations have been discussed, Table 3 shows balloon parameters and values calculated using the equations discussed in this section for the flights in this project. Weather data are also displayed, where data at the surfaces were taken using a Kestrel Weather Meter on a rotating tripod, and

Table 2.2: Balloon parameters and calculated float parameters for the pico balloons used in this study. Atmosphere surface data are from measured data from Kestrel Weather Meter and data at float are from station 12 UTC sounding.

Balloon Parameters							Weather at Surface			
Callsign	Time Launched	Float altitude after launch	Payload Mass	Free Lift	Neck Lift	Ascent Rate at 6km Altitude	T	P	WS	WD
	UTC	m	g	g	g	m s^{-1}	°C	mb	kts	deg
K4UAH-3	13.11.2022 14:19:00	11125	13.12	7.00	20.12	0.95	-15	961	10	250
K4UAH-1	16.11.2022 10:28:00	10900	15.8	7.00	22.80	0.87	-5	985	5	121
W5KUB-114	16.11.2022 11:06:00	10665	19.25	8.00	22.80	1.00	-5	985	7	96
K4UAH-2	20.11.2022 7:44:00	11071	15.47	7.00	22.47	0.97	-11	983	2	96
K4UAH-4	20.11.2022 8:10:00	11139	15.85	7.00	22.85	0.98	-10	983	0	-
K4UAH-6	20.11.2022 8:30:00	10834	18.55	7.00	25.55	1.00	-12	983	3	113
W5KUB-115	23.11.2022 8:26:00	10696	22.5	8.00	30.50	1.08	-5	982	1	-
K4UAH-5	29.11.2922 11:18:00	11240	15.88	7.00	22.80	0.95	-3	978	2	68
Calculated Float Parameters							Weather at Float			
Callsign	Estimated Float Density	Actual Float Density	Float Density Percent Error	Mass of Balloon System	Volume of Balloon	Estimated Balloon Pressure	T	P	WS	WD
	kg m^{-3}	kg m^{-3}	%	g	m^3	psi	°C	mb	kts	deg
K4UAH-3	0.319	0.317	0.6	63.77	0.2	0.326	-69	186	5	328
K4UAH-1	0.340	0.34	0.1	66.88	0.2	0.226	-66	202	51	220
W5KUB-114	0.335	0.354	0.3	71.05	0.2	0.462	-67	210	49	220
K4UAH-2	0.333	0.333	0.1	66.5	0.2	0.333	-67	197	44	245
K4UAH-4	0.355	0.325	3.1	66.94	0.2	0.409	-67	193	43	245
K4UAH-6	0.350	0.342	2.3	70.07	0.2	0.424	-66	203	45	240
W5KUB-115	0.374	0.356	5.1	74.66	0.2	0.450	-69	209	40	249
K4UAH-5	0.335	0.335	0.1	66.98	0.2	0.216	-75	191	32	275

weather at float was determined using the Neumayer Station 12UTC sounding. To compare estimated and actual float densities, pico balloon GPS altitudes were paired with GPS sounding altitudes, and density was calculated using the sounding pressure and temperature using Equation 5. We find for most of the balloons, estimated float densities are very close to the actual float density (less than 6-percent error). It has been observed that an increase in lifting gas used in the balloon results in a higher percentage of error in estimating the float density, as shown in Table 3. The W5KUB-115 balloon, which had the heaviest payload and higher free lift value, showed a float density percentage error of 5.1-percent. This discrepancy could be explained by an increase in V_f during the transition to float, causing the balloon membrane to stretch farther and resulting in a higher float density than predicted, as observed in this particular flight. We also see that the K4UAH-5 balloon was unfortunately the only one that did not reach a safe float, as it leaked and descended only three hours after floating at 11.2 km. This serves as a reminder that despite following all procedures correctly, the cheap quality of party balloons does not guarantee a 100-percent success rate.

2.3 Pressure Testing

To determine how a balloon will perform at float altitude, it is important to understand the limits of the balloon envelope. By subjecting a pico balloon to pressure testing, we can gain insight into the forces it can withstand. A typical pressure testing lab is shown in Figure 2.1. Using compressed air, the pico balloon can be filled to a pressure determined by a manometer. A small pressure release

tube is included to allow for quick venting once the target pressure is met. The first variable needed to understand the limit of the pico balloon is the burst pressure, P_b. This is found by simply filling the balloon envelope until burst. It is better to do this test multiple times to get a range of P_b values to quantify uncertainty and reliability of the pico balloon. Once P_b has been found, the optimal pressure test range can be found.

For pico balloons, which are defined by a 0.5 to 2 meter diameter, the optimal pressure range is often a little more (for our balloons, +0.33 psi) than $P_b/2$. A pressure test diagram for the balloons used in this project is detailed in Figure 2.2. For our pico balloons, P_b was found to be 0.728 psi. Using the $P_b/2$ rule, we find that the best pressure test for this project's balloons is around 0.4 psi; in this project, all pico balloons were pressure tested to 0.4 psi, where the balloon pressure was brought to 0.4 psi and the vented to 0.3 psi using the pressure release tube.

Figure 2.2 also shows the safe, risky, and unsafe pressure testing ranges. The general rule of thumb is one should stretch the balloon envelope enough that it will not burst once it is expanding during ascent, but not stretch it so much that it will easily reach P_b during its flight time. The balloon can reach P_b when encountering strong density gradients and/or updrafts that pierce the tropopause into the lower stratosphere. Therefore, it's optimal to be below P_b to give it room to stretch if needed. Also note that the balloon envelope will stretch over time, meaning your flight will be limited if your pressure test range is too close to P_b. Another important factor is ensuring the balloon is fully pressurized at

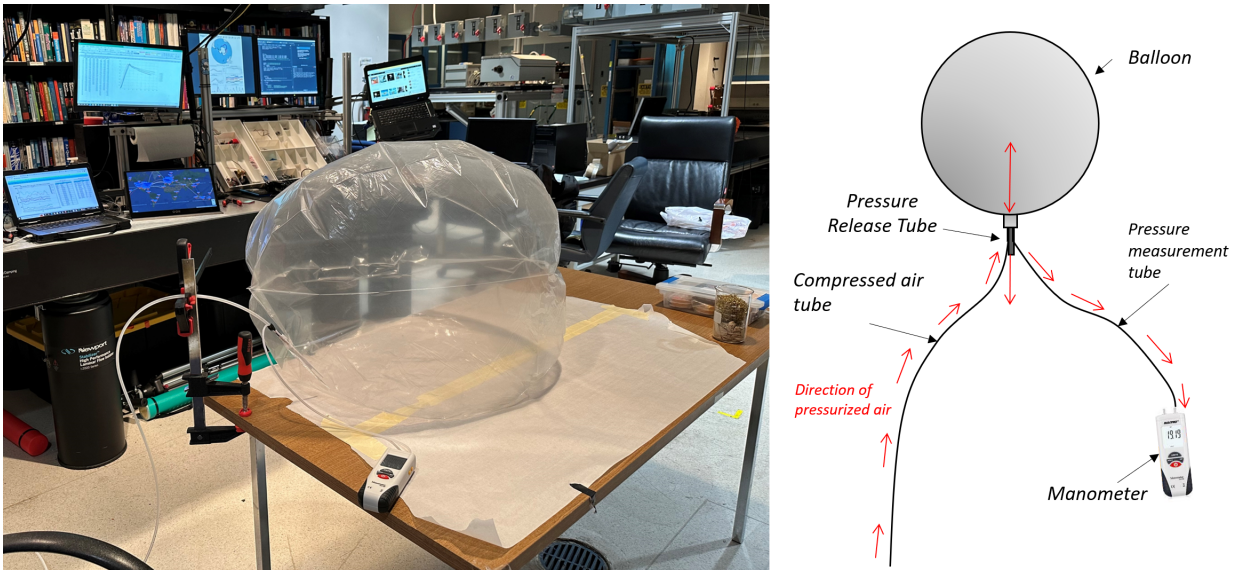

Figure 2.1: Typical pressure test lab with compressed air tube balloon schematic.

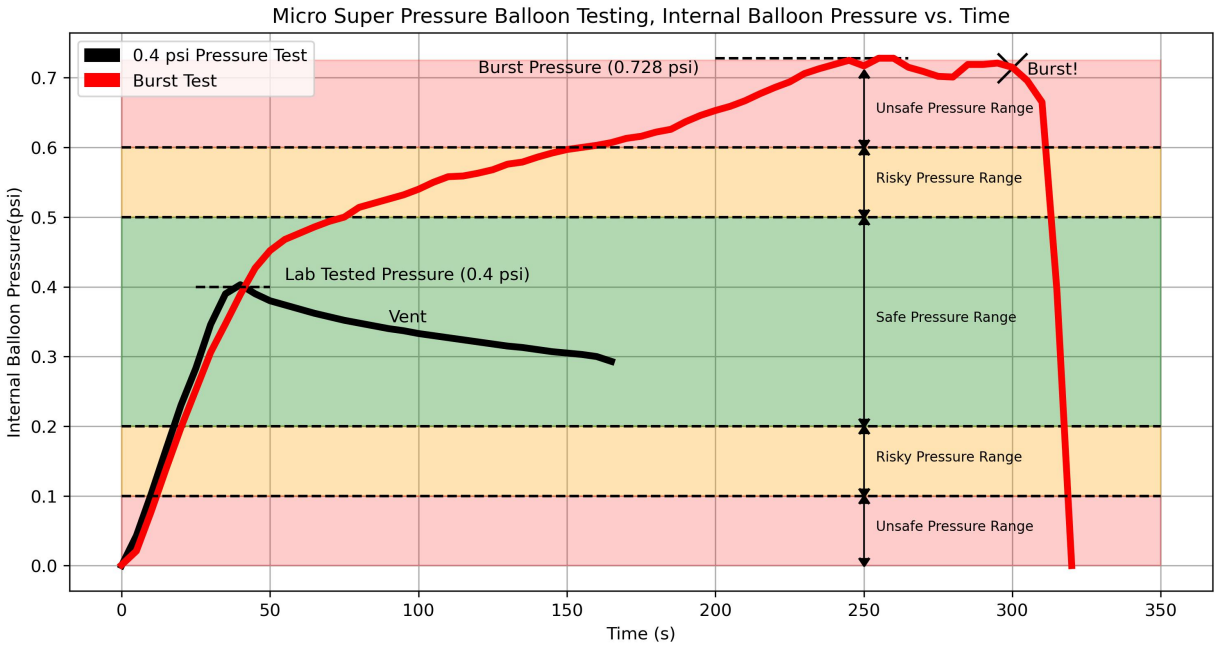

Figure 2.2: Lab pressure curves vs. time for lab tested balloon and a burst balloon. Safe pressure testing ranges are notated with arrows and green color. All balloons are pressured tested to 0.4 for this study.

float. Pico balloons oscillate vertically while floating; if the pico balloon is not fully pressurized, the lifting gas inside will adiabatically expand and contract the balloon membrane repeatedly. This quickly stresses the balloon envelope until it forms leaks.

2.4 Success Criteria

In order to evaluate the potential for successful deployment pico balloons, a "Likelihood to Succeed (LTS) Chart" can be created. This chart is generated by combining various factors such as balloon burst pressure, atmospheric parameters at float, amount of lifting gas, and free lift. This graphical representation, shown in Figure 2.3, illustrates the relationship between free lift and calculated internal balloon pressure, with the inclusion of burst pressure and the $P/2$ rule. The calculated balloon parameters for this project are also plotted on the chart as represented by an X. The high, low, and risky ranges on the chart are derived from the scale introduced in Table 2.1 and Figure 2.2. In this specific project, it was observed that two of the balloons were on the high-to-moderate line due to their heavier payloads and a 1-g higher free lift as compensation.

Additionally, a flow chart in Figure 2.2 outlines the recommended process for pico balloon testing, starting with inputs such as payload mass, balloon size, and lifting gas, and utilizing the equations previously discussed to calculate the estimated float density and internal balloon pressure at float. By following these processes, any small balloon, whether purchased or made from scratch, can be evaluated and tested to predict its potential as a pico balloon.

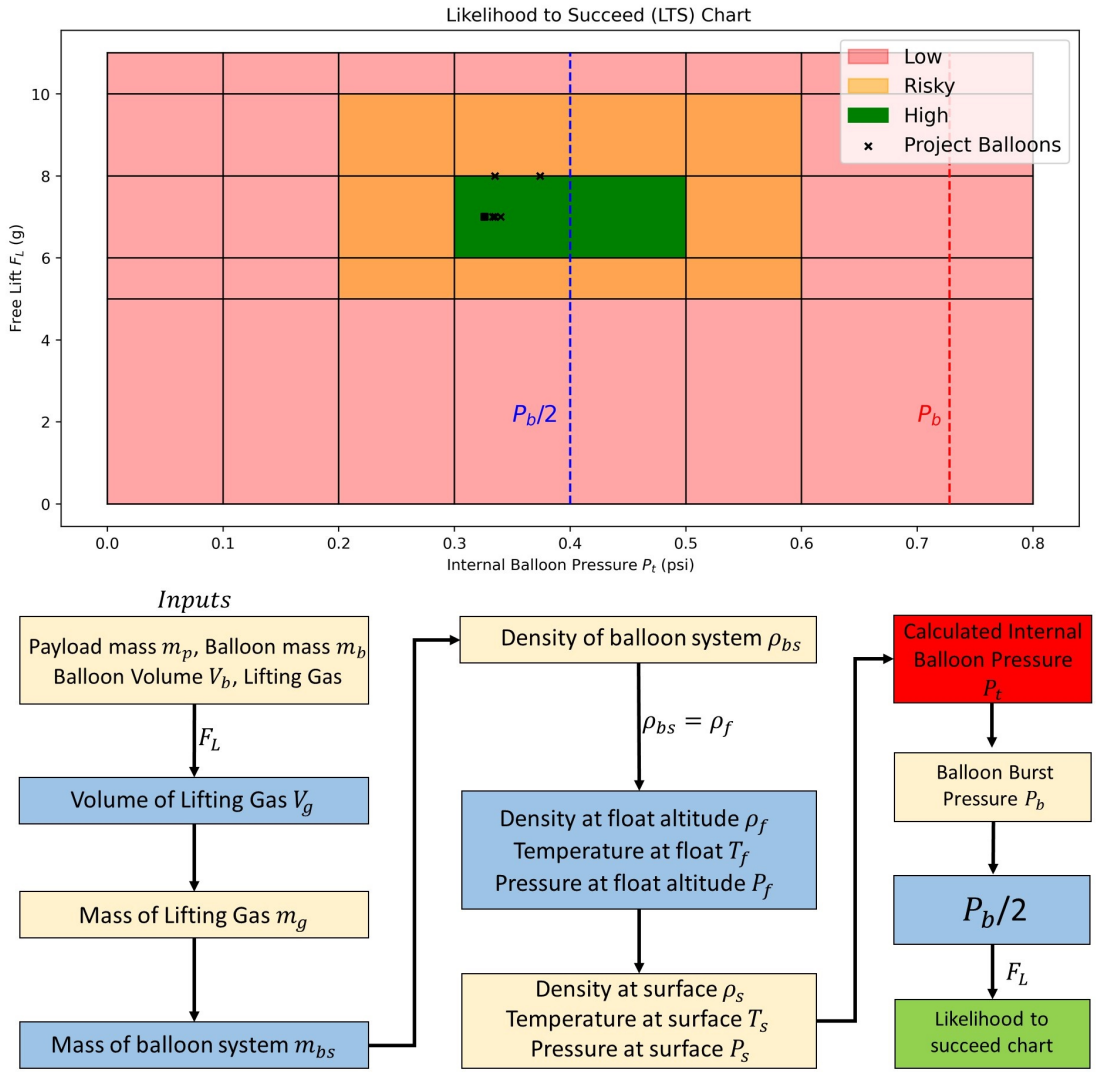

Figure 2.3: Likelihood to Succeed chart and flow chart summarizing the pico balloon equations. The X points show the values for the balloons used in this study. The P_b and $P_b/2$ pressures are plotted with dotted lines. The high, low, and risky ranges on the chart are derived from the scale introduced in Table 2.1 and Figure 2.2.

Chapter 3. Transmitting Data from Pico Balloon Flights

The weight limitations of pico balloons are quite restrictive, with payloads commonly limited to below 50 g. This represents the main drawback of these balloons compared to larger SPBs, which can support heavier payloads that typically use sophisticated communication systems such as Iridium modems [21] or other high-power, over-the-horizon communication technologies [30]. In this project, the balloons utilized an amateur radio protocol called the Weak Signal Propagation Reporting (WSPR) system [29], with each payload weighing below 31 g. This balloon-based telemetry system is discussed in detail in [18] and relies on ground stations operated by amateur radio enthusiasts around the world. Data transmission in this study was achieved through payloads that utilized the 20 meter (≈14.09 MHz) band. This band offers long-range telemetry capabilities, with some balloon data being received from distances up to 18,000 km away. Furthermore, apart from its primary use as a telemetry communication method, this technique can also serve as a means to profile ionospheric propagation on a broader scale; the results from these flights in the context of ionospheric propagation are presented in [19]. An example transmission from one of the balloons is shown in Figure 3.1, where telemetry data were sent to stations in Australia, the United States, South America, Africa, and Norway. In addition, a WSPR station

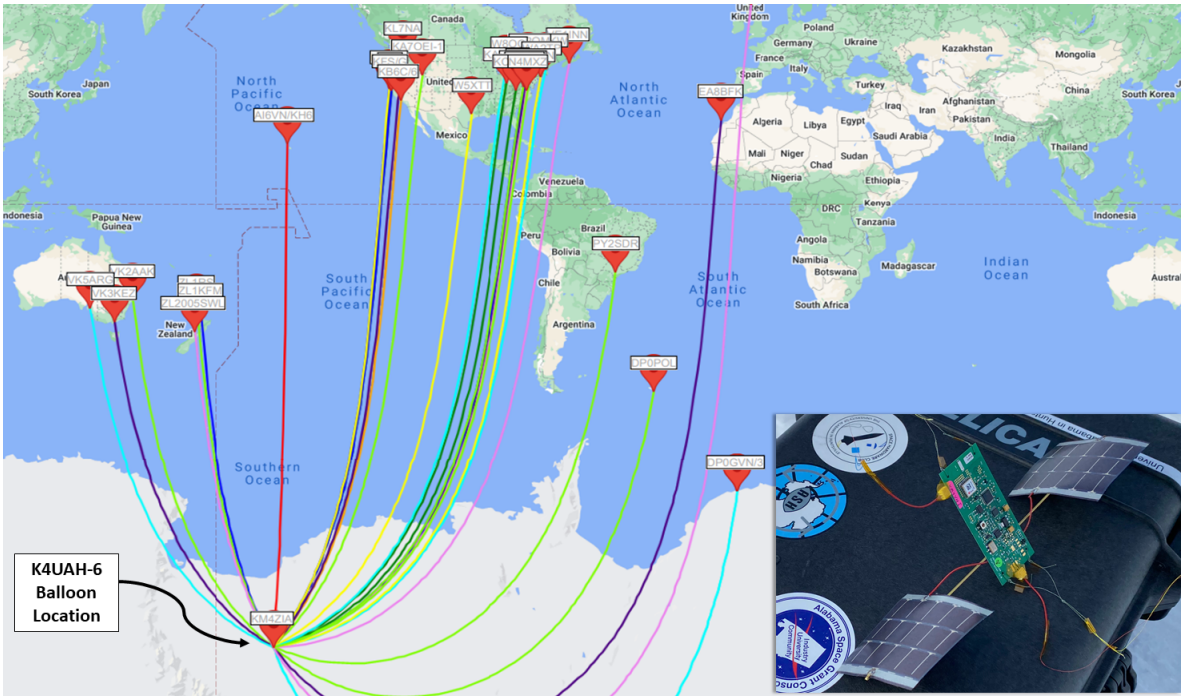

Figure 3.1: Typical WSPR transmition range over Antartica. The balloon location at the time of these transmissions is notated. The WSPR SkyTracker is shown in the bottom right photograph. The stations receiving the balloon transmissions are shown by a call sign identifier and red marker.

set up at Neumayer Station III [13] has commonly received balloon telemetry for all the flights.

A picture of one of the WSPR payloads, called the SkyTracker [5] , is also shown in Figure 3.1. WSPR trackers manufactured by the W5KUB group [31] and the Northern Illinois Bottlecap Balloon Brigade [20] were also deployed. It is important to note that these trackers are solar powered only, meaning they do not transmit during the nighttime; during Antarctica summer, while flying over the continent, some flights were observed to transmit 24/7 due to the polar day. The data that can be sent from these flights are limited due to the both the

transmission protocol and the weight limit of the payloads. For these flights, the following information was transmitted from each balloon payload: latitude and longitude, altitude, solar voltage, and satellite lock. Wind speed and direction can be calculated from GPS position. The development of low cost/ lightweight payloads that can support more instrumentation will define the next decades of pico balloons.

Chapter 4. Filling and Launch

Filling a pico balloon requires a high degree of precision due to the small amount of lifting gas used. Overfilling or under-filling the balloon can greatly impact its performance and stability, leading to a short flight time. The amount of lift needed for a pico balloon is given by the neck lift (N_L), with

$$N_L = F_L + m_p, \tag{4.1}$$

where the mass of the payload m_p and neck lift N_L are in g.

With no payload attached, N_L values above zero ($N_L > 0$) will cause the balloon to rise. The neck lift values used in this project are shown in Table 3, which range between 20.15 to 30.50 g. To give context for how little this is, a typical National Weather Service weather balloon has a N_L of around 1000 g.

For pico balloons, N_L is measured using a jewelry gram scale that measures out to two decimal places. A weight is tared to the scale and the balloon is hooked onto the weight to measure the lift. It is imperative that the balloon-fill room has little to no airflow (*i.e.*, no open window breeze, no direct AC/heating unit airflow), as this can reduce the reliability of the N_L measurement. Once the balloon has been filled, it is often sealed with a heat iron and Kapton tape, and the payload is attached to the neck of the balloon.

There are few environmental factors to consider when launching pico balloons. Pico balloons can be launched in wind speeds faster than requirements set by larger SPBs flights, with a max wind of 22 km hr^{-1}. Another crucial factor to consider is moisture in the atmosphere. Moisture poses several challenges for pico balloons, such as the formation of ice on the balloon surface, which can increase its weight and lead to a decrease in altitude. To prevent these problems, it is advisable to release pico balloons on days with clear skies or thin cloud cover. This will help ensure that the balloon does not accumulate ice. Figure 4.1 shows the ascent rates of the pico balloons. Overall the ascent rate gradually increase until the balloon nears its float altitude which occurs after approximately 170 minutes. This qualitatively agrees with the dynamic model in [35] which assumes constant C_{D}. The relatively large variation of ascent rates below 3000 m may be due to meteorological conditions in the mixing layer as well as changes in the drag coefficient C_{D} which depends on shape and Reynolds number. At the surface, the balloon appears barely inflated and resembles a wrinkled grocery bag. It assumes a more spherical shape as it ascends.

After launch, it is advisable to check the balloon ascent rate at a certain altitude. For a pico balloon, the ascent rate should be be between 0.80 to 1.1 m s^{-1} at 6 km. If the ascent rate is higher than this range, there is a very high likelihood that the balloon will burst while trying to achieve float. As previously mentioned, when a balloon exceeds its expected float altitude, the balloon material may stretch excessively, resulting in leaks or ruptures. This danger is intensified by higher free lifts, as the external pressure decreases with increased altitude, causing

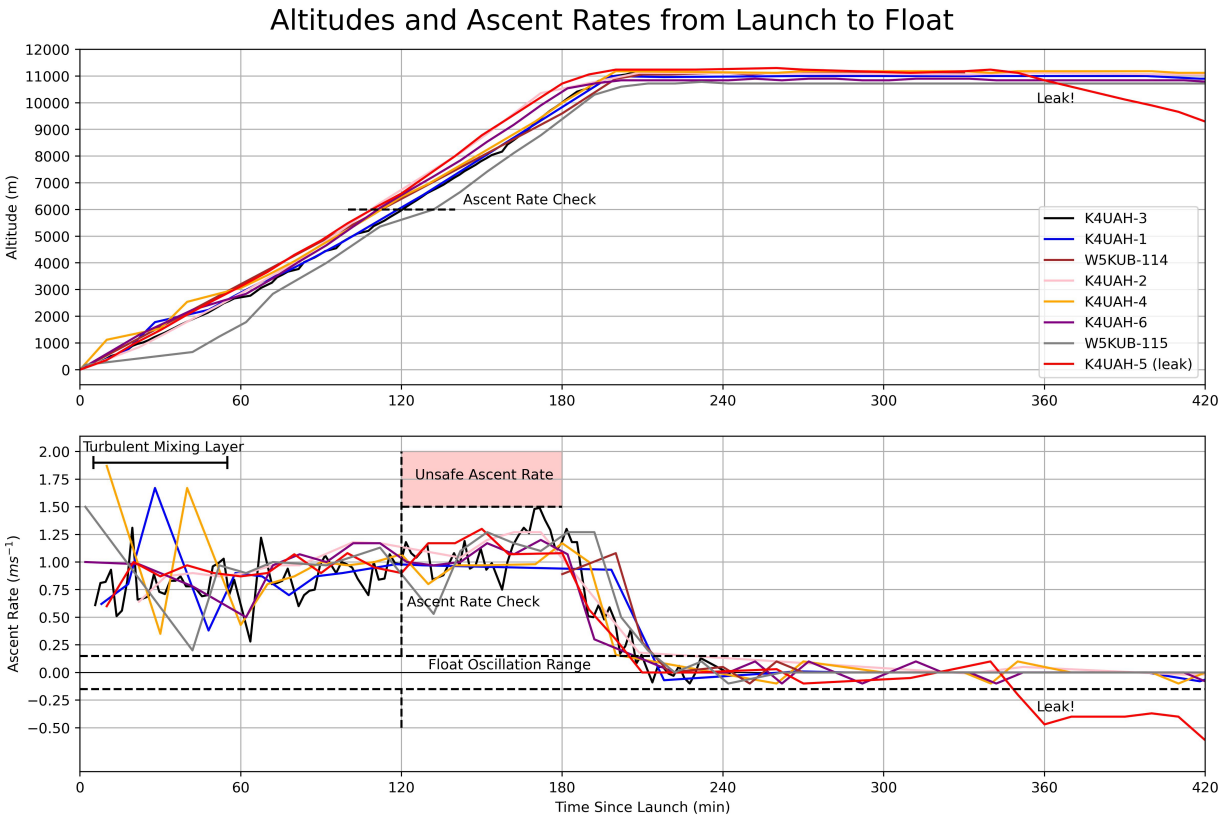

Figure 4.1: Balloon ascent rates on launch day. Float range and ascent rate checks are notated. Assent rates above 3000 m have less variance.

higher pressure inside the balloon and pushing it closer to its bursting limit. The ascent continues until the buoyant force and the gravitational force balance resulting in no net force on the balloon. Here it will enter the "float oscillation range" (as shown in Figure 4.1, between -0.2 and 0.2 m s^{-1}) and behave like an air parcel floating on a constant density surface.

Chapter 5. Long Term Flight Performance

The following discussion will focus on the results achieved from balloons that remained aloft for extended periods of time. The balloons K4UAH-5 and K4UAH-3, which encountered factors such as a premature leak and limited range radio tracker, respectively, will not be included in this analysis. Instead, we will highlight the exceptional performance of the six successful balloons, each with a flight duration surpassing 30 days. The longest-flying balloon achieved a remarkable 98 days aloft, completing eight circumnavigations of the Southern Hemisphere. Figures 5.1 and 5.2 present the trajectories and altitudes, latitudes, speeds, and zonal and meridional velocities of the balloons.

5.1 Flight Velocities and Latitude Range

Balloon altitudes ranged from 10 to 12.5 km AMSL, and it was observed that altitude generally increased over time as they drifted farther from the colder, denser Antarctic region. Mean zonal velocities were between -50 and 250 km hr^{-1} and meridional velocities $\pm$100 km hr^{-1}. Total wind speeds range from 2.0 to 270 km hr^{-1}. This range of velocities are much different from winds measured from larger-higher flying SPBs. For example, the Vorcore SPB campaign measured winds between altitudes of 17 to 19 km and found meridional winds being in the

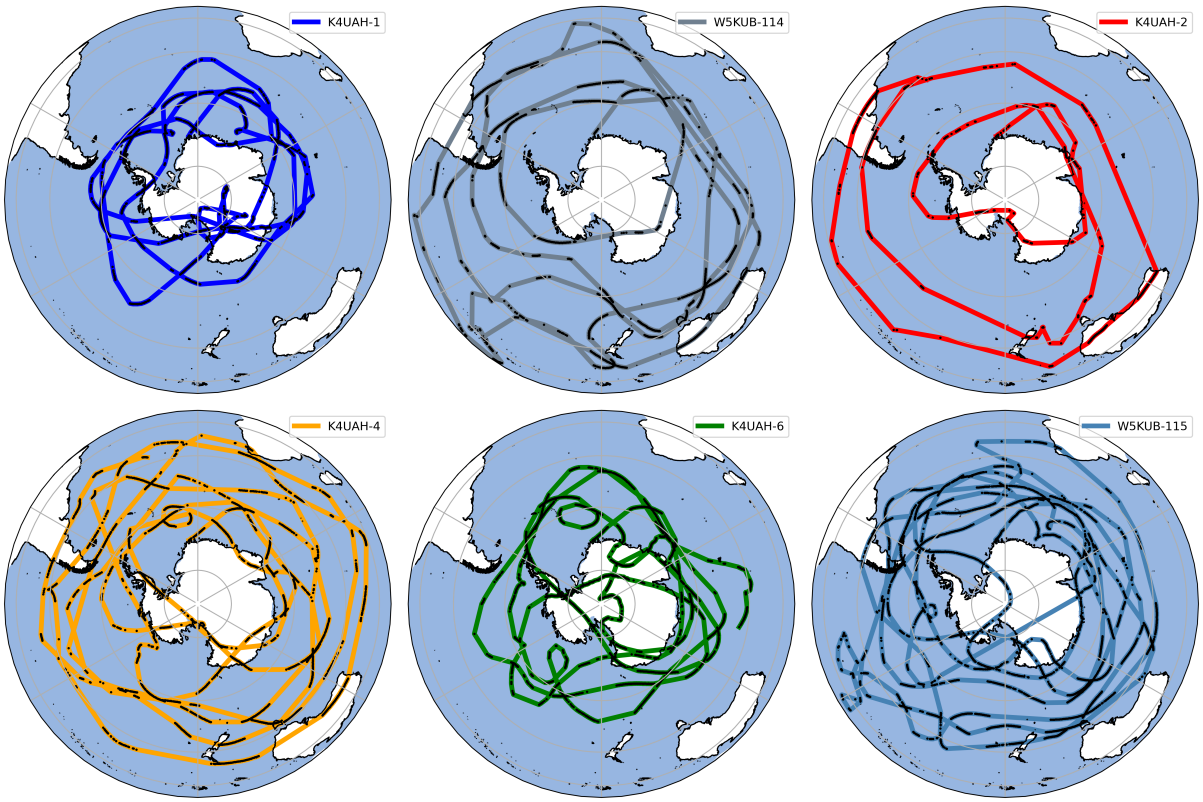

Figure 5.1: Polar maps showing six of the long duration balloon flights. The black dots over the flight paths show points when the balloon transmitted a data point. Colored lines are linearly interpolated between black dots.

range of ±61.2 km hr^{-1} and zonal velocities mostly within a range of 3.6–158.4 km hr^{-1} [2]. In addition, the transition from slower polar air masses to fast jets between latitudes 60°S and 50°S was observed, and this transition was found to have a significant impact on the motion of the pico balloons. Sharp gradients in wind speed at these heights could quickly accelerate or decelerate the balloons. In certain instances, balloons would become trapped in polar lows, where they would persist within the low pressure systems until the arrival of a new trough with strong and accelerated zonal winds. Rarely seen in the larger, higher-flying SBS flights that typically experience dominant zonal winds, these occurrences offer a valuable data set for future trajectory modeling studies in the upper troposphere and lower stratosphere.

The latitude range of the pico balloons flights in this study differs significantly from that of typical large scale stratospheric balloon flights. [11] conducted an in-depth analysis of the flight paths of 40 larger stratospheric balloons launched from McMurdo Station between 1991 and 2020. The balloons floated at altitudes ranging from 30 to 40 km. They found that with median flight duration of 18 days, there is a probability of 10 percent or less that the balloons would drift as far south as 88°S or as far north as 71°S. The balloon flights floating lower also had a clear tendency to drift north relative to the flights floating higher. The pico balloons launched in this study quickly exceeded the probabilistic bounds after 18 days outlined in [11], where balloons K4UAH-6, and W5KUB-115 made impressive journeys to the 88°S line before the 18 day mark. This observation supports the idea that balloons at lower altitudes are more likely to encounter

higher variability in their latitudinal floating range, in contrast to previous larger SBS flights that were launched deeper within the polar vortex.

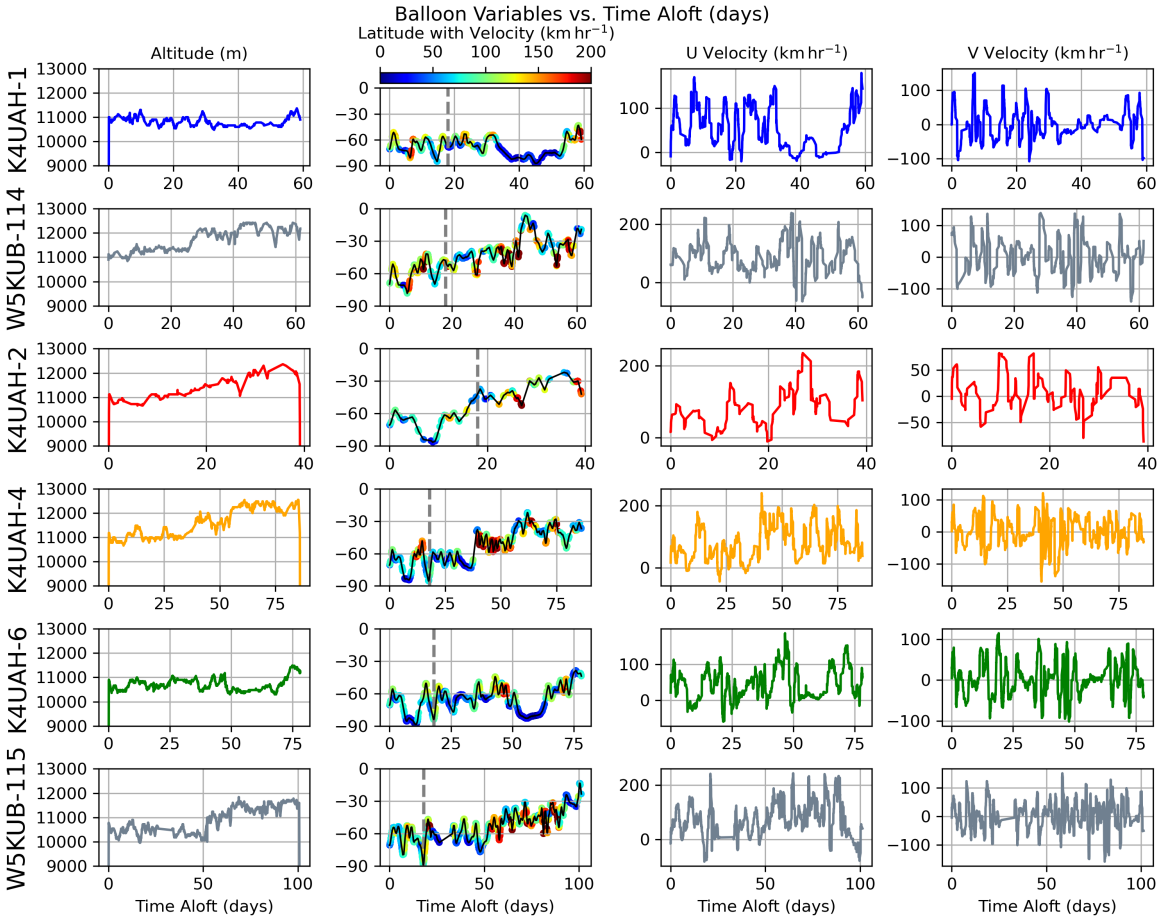

Figure 5.2: Balloon data from the six long-duration flights. Altitudes are in AMSL. Latitude vs. time plots are colored by the speed of the balloon. Altitudes, U, V line plots correlate to the colors on Figure 7. The dotted dashed gray line on the latitude plots represents the 18 day mark outlined in [11].

5.2 Float Altitudes and Convection

We can investigate whether and how often changes in the balloon's altitude are due to convection by looking at the float density calculated from the pressure and temperature at the balloon altitude and the surface-based Convective Available Potential Energy (CAPE) and the Equilibrium Level (EL). CAPE quantifies the potential energy available to a specific air parcel when surrounded by an ambient environment. The EL indicates the altitude to which a potentially buoyant air parcel may ascend before reaching an equilibrium state and discontinuing its upward trajectory. We specifically aim to examine variations in float density caused by thermodynamic events, independent of changes in balloon system density (although thermodynamic events may influence balloon system density). For the analysis here, the National Oceanic and Atmospheric Administration (NOAA) HYSPLIT model [26] and its interpolation routines using the Global Data Assimilation System (GDAS) 1.0° meteorological model, we found pressure, temperature, CAPE and EL along the balloon's flight path.

In general the balloons float on a constant density surface so that changes in altitude mostly reflect changes in pressure and temperature. Deviations from the constant density surface can occur for two reasons. The density of the balloon system may change by losing mass to a leak, gaining mass due to icing, or increase in volume due to stretching of the balloon material. The balloon can also be temporarily pushed off of the constant density surface by a thermodynamic event (*e.g.* latent heat release, downdraft, updraft). After such a displacement

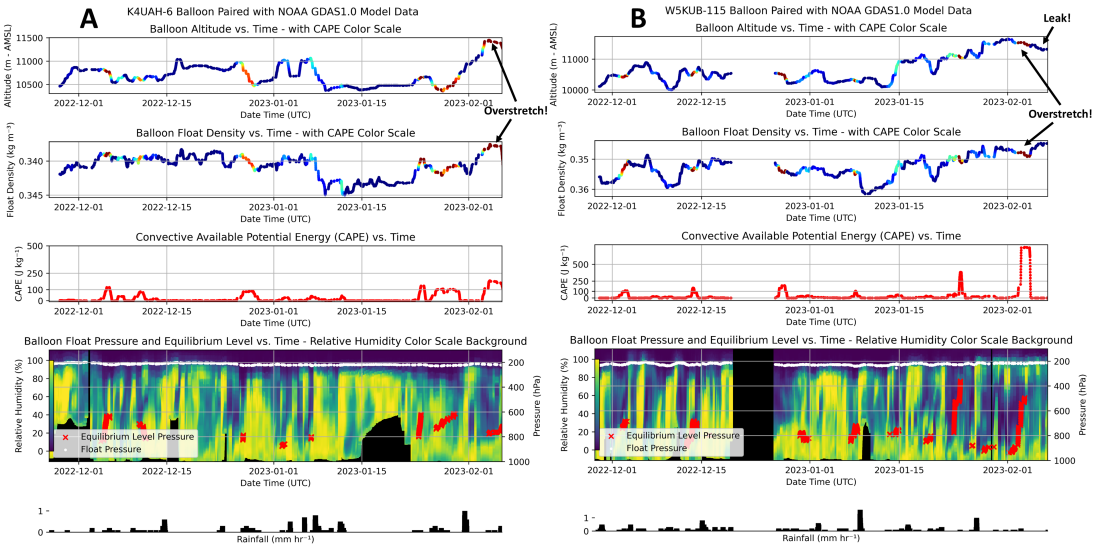

Figure 5.3: Two balloons in relation to NOAA GDAS1.0 model float density, CAPE, float pressure, and rainfall during their flights. Data are plotted over time in UTC. A color scale representing model relative humidity overlays the pressure versus time plot (the model profile under each balloon), with black areas indicating missing data or terrain. The red 'X' symbol denotes the Equilibrium Level pressure height. The first two plots—float altitude and float density—are color-coded according to the CAPE values. A) The K4UAH-6 balloon exhibits an elevation increase towards the end of its flight, potentially leading to overstretch and flight termination. B) The W5KUB-115 balloon's flight demonstrates an increased float altitude (and corresponding decrease in float density), indicative of a leak that caused it to descend.

the balloon often simply returns to its original state and float density. If the displacement is large enough, the increased differential pressure experienced by the balloon may lead to stretching and permanently increased volume of the balloon and subsequently lower float density. This can also cause leaking or bursting of the balloon. Indeed, most of the pico balloon failures are associated with large convective systems in regions with high moisture levels. Seven of the eight balloons in this study terminated their flights while traversing maritime convection zones within latitudes 40°S to 30°S. It is also noteworthy that float density exhibits less variability when the balloon is navigating through dry atmospheres; this was especially apparent when flying over Antarctica, which experienced little to no surface-based CAPE and low humidity at float altitudes. We plot two examples in Figure 5.3, where we show model convective parameters versus time for the W5KUB-115 and K4UAH-6 balloon. Note that for both flights, the balloons experienced a decrease in float density when CAPE was above 100 J kg^{-1}. We believe that in both of these cases the balloon membrane was permanently stretched and damaged, resulting in leaking and termination of the flight.

We show another figure, Figure 5.4, which presents a scatter plot depicting EL density heights against the change in balloon density for the six balloon flights. We illustrate scenarios where the balloons were positioned over regions with either no CAPE, indicating minimal or no convection (*i.e.*, low EL heights), and regions where there was a substantial CAPE (>1000 J kg^{-1}) with high EL heights. In Figure 5.4, we observe that, up to EL density heights of 0.6 kg m^{-3}, the change in balloon float density remains relatively unchanged due to the convec-

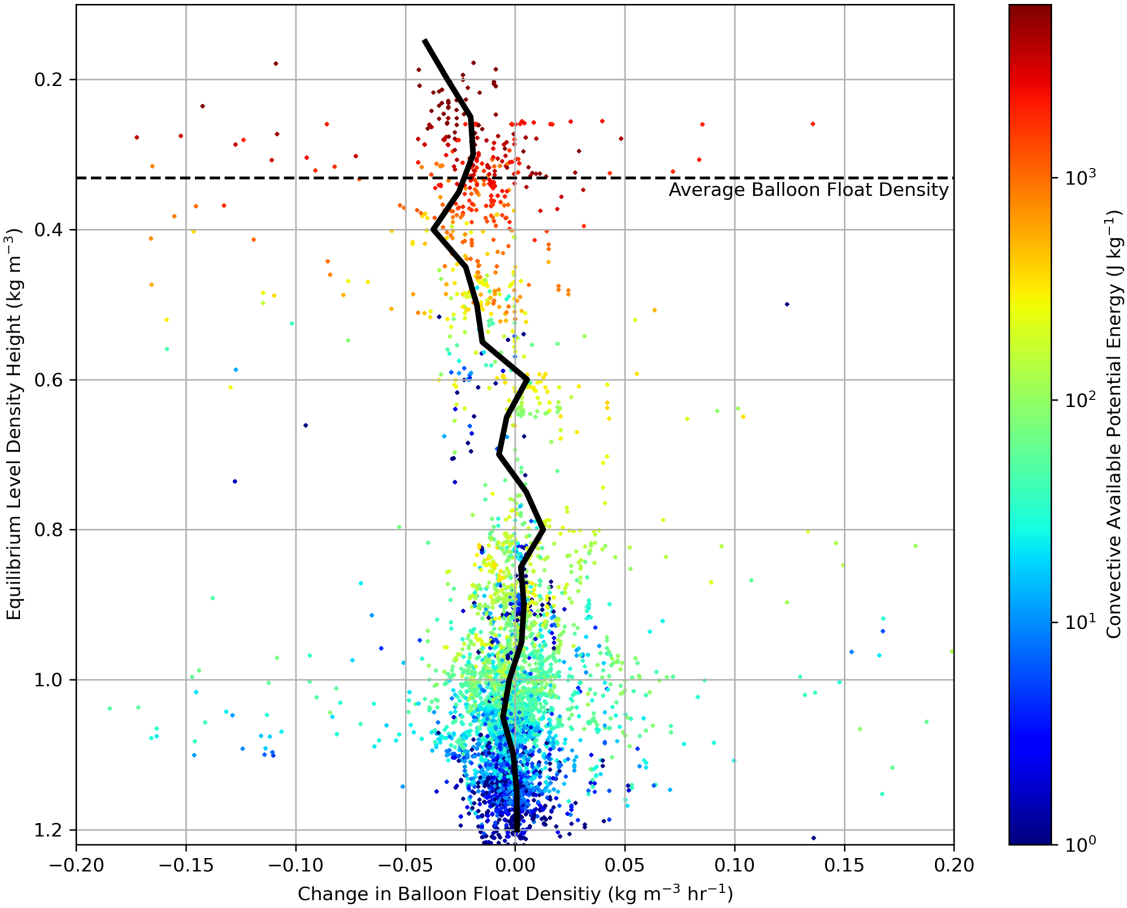

Figure 5.4: Equilibrium level (EL) density height versus the change in balloon float density over time. Scatter points are colored by the model surface-based CAPE. A mean profile line is plotted by a black line at 0.05 kg m^{-3} bin sizes. The average float density for the balloons is plotted with a horizontal dashed line. Shows that at 0.6 kg m^{-3} EL density height, float density on average decreases with decease in EL density (*i.e.,* increase in EL altitude.)

tion underneath the balloon. This suggests that in these cases, the tropospheric air parcels lack sufficient buoyant force to ascend to higher altitudes, resulting in negligible alterations to the balloon float densities. However, starting at an EL density heights of 0.6 kg m^{-3}, a noticeable change in balloon density occurs, indicated by a decreasing mean line in Figure 5.4. This indicates that, on average, pico balloons' floating behavior is influenced by higher-level convection when EL density heights are below 0.6 kg m^{-3}. Given the complicated thermodynamic nature of the atmosphere, particularly near the troposphere-stratosphere boundary, and the lower resolution of the global model (1° grid), we believe this analysis reveals a robust correlation between pico balloon float densities and higher EL heights. Apart from this publication, which primarily focuses on methodology, future studies would benefit from calculating CAPE and EL from different heights to enhance this analysis. Additionally, incorporating high-resolution pressure, humidity, and temperature sensors on future balloon flights, along with comparing the data to higher-resolution models, would substantially contribute to furthering this investigation.

Chapter 6. Conclusions and Future Work

We have demonstrated that pico balloons have remarkable capabilities for conducting long-duration and high-altitude flights, and are able to survive Antarctic conditions. The ability to operate at high altitudes for long periods, coupled with their low cost, makes pico balloons an attractive platform for a wide range of scientific and commercial applications, such as weather monitoring, atmospheric research, and signal-propagation research. By demonstrating the pressure-testing process and deployment techniques for pico balloons, these techniques can be applied to party or homemade balloons to assess their success rate based on factors such as payload mass, lifting gas quantity, and balloon characteristics. Furthermore, the six longer-duration balloon flights from this study have captured unique wind patterns around Antarctica that are not accessible by large SPBs. We have also characterized the influence of convection and identified potential benefits of evaluating the float altitude of pico balloons. The promising performance of pico balloons over long durations and distances bodes well for future applications and targeted experiments. By utilizing these low-flying balloons, it could be possible to deepen the understanding of the dynamic interactions between the surface and the atmosphere, which can give rise to atmospheric waves [8]. Additionally, the transport of ozone across the global stratosphere-troposphere boundary could

be evaluated using pico balloon-sized instrumentation [28]. Being aware of the distinctive characteristics of pico balloons is crucial for users to maximize their capabilities. When adequately prepared, these balloons can achieve flight durations that rival those of multimillion-dollar SPB projects. For instance, during the Vorcore campaign, out of the 25 balloons that floated, the average flight duration was 63 days [14]. In comparison, the average flight duration for the pico balloon flights conducted in this study was 69 days. The biggest downside of pico balloons is the extreme mass limitation of the payloads. Therefore, we strongly emphasize the importance of developing low-cost, lightweight instrumentation that can be flown on pico balloons. Standardizing sensors for pico balloons will mark the next phase of SPB research. Promising results obtained from simulating a fleet of stratospheric balloons indicates that a constellation of such balloons in the global observation system is both feasible and advantageous to the scientific community [17]. As pico balloons become more common in the scientific community, clearly defined international collaborations will be advantageous [16]. The data collected in this study have implications for other scientific investigations, such as the evaluation of NOAA HYSPLIT trajectories, as demonstrated in [18], and the assessment of WSPR propagation in lower latitudes [19]. Furthermore, these affordable balloons could serve the purpose of validating wind measurements taken from space-based observation systems, such as the AEOLUS Doppler lidar, in remote regions [23, 27]. By advancing research with pico balloons, it is possible that these balloons could provide a cost-effective method of collecting data in the upper atmosphere of other planets [24, 1, 12]; pico balloons are also much more

compact and lightweight than traditional SPBs, making them easier to transport and store during spaceflight. We plan to continue deploying and analyzing pico balloons to demonstrate their potential as a valuable meteorological asset and work towards worldwide standardization of pico balloon use.

References

[1] JE Blamont, RE Young, A Seiff, B Ragent, R Sagdeev, VM Linkin, VV Kerzhanovich, AP Ingersoll, D Crisp, LS Elson, et al. Implications of the vega balloon results for venus atmospheric dynamics. *Science*, 231(4744):1422–1425, 1986.

[2] G Boccara, A Hertzog, C Basdevant, and F Vial. Accuracy of ncep/ncar reanalyses and ecmwf analyses in the lower stratosphere over antarctica in 2005. *Journal of Geophysical Research: Atmospheres*, 113(D20), 2008.

[3] D Ray Booker and Lynn W Cooper. Superpressure balloons for weather research. *Journal of Applied Meteorology and Climatology*, 4(1):122–129, 1965.

[4] Bill Brown. Send an amateur radio high altitude balloon around the world. In *Academic High Altitude Conference*, volume 2020. Iowa State University Digital Press, 2022.

[5] Bill Brown. Wb8elk skytrackers, 2023. Accessed 5 February 2023, url = https://gmigliarini.wixsite.com/wb8elk.

[6] H. M. Cathey. The NASA super pressure balloon - a path to flight. *Advances in Space Research*, 44(1):23–38, 2009.

[7] Stephen A Cohn, Terry Hock, Philippe Cocquerez, Junhong Wang, Florence Rabier, David Parsons, Patrick Harr, Chun-Chieh Wu, Philippe Drobinski, Fatima Karbou, et al. Driftsondes: Providing in situ long-duration dropsonde observations over remote regions. *Bulletin of the American Meteorological Society*, 94(11):1661–1674, 2013.

[8] Christian Ethé, Claude Basdevant, Robert Sadourny, KS Appu, L Harenduprakash, PR Sarode, and G Viswanathan. Air mass motion, temperature, and humidity over the arabian sea and western indian ocean during the indoex intensive phase, as obtained from a set of superpressure drifting balloons. *Journal of Geophysical Research: Atmospheres*, 107(D19):INX–22, 2002.

[9] FAA. Part 101—moored balloons, kites, amateur rockets, and unmanned free balloons, 2021. Accessed 1 February 2023, https://www.ecfr.gov/current/title-14/chapter-I/subchapter-F/part-101.

[10] Leon S Friedrich, Adrian J McDonald, Gregory E Bodeker, Kathy E Cooper, Jared Lewis, and Alexander J Paterson. A comparison of loon balloon observations and stratospheric reanalysis products. *Atmospheric Chemistry and Physics*, 17(2):855–866, 2017.

[11] Christopher Geach, Shaul Hanany, Chiou Yang Tan, and Xin Zhi Tan. Trajectories of long duration balloons launched from mcmurdo station in antarctica. *Journal of Astronomical Telescopes, Instruments, and Systems*, 7(2):027002–027002, 2021.

[12] Jeffery Hall, Michael Pauken, Viktor Kerzhanovich, Gerald Walsh, Debora Fairbrother, Chris Shreves, and Tim Lachenmeier. Flight test results for aerially deployed mars balloons. In *AIAA Balloon Systems Conference*, page 2626, 2007.

[13] Michael Hartje and Ulrich Walter. Wspr radio beacon at neumayer station iii for evaluation of southern hemisphere radio propagation. *zur Polar-und Meeresforschung Reports on Polar and Marine Research*, page 42, 2020.

[14] Albert Hertzog, Philippe Cocquerez, René Guilbon, Jean-Noël Valdivia, Stéphanie Venel, Claude Basdevant, Gillian Boccara, Jérôme Bordereau, Bernard Brioit, François Vial, et al. Stratéole/vorcore—long-duration, super-pressure balloons to study the antarctic lower stratosphere during the 2005 winter. *Journal of Atmospheric and Oceanic Technology*, 24(12):2048–2061, 2007.

[15] Naoki Izutsu, Daisuke Akita, Hideyuki Fuke, Issei Iijima, Yoichi Kato, Jiro Kawada, Kiyoho Matsushima, Yukihiko Matsuzaka, Eiichi Mizuta, Takashi Nakada, et al. Development of a super-pressure balloon with an improved design. *Transactions of the Japan Society for Aeronautical and Space Sciences, Aerospace Technology Japan*, 8(ists27):7–13, 2010.

[16] W Vernon Jones. Global balloon flight obstacles and opportunities. *Advances in Space Research*, 33(10):1600–1607, 2004.

[17] A. Keil. Assimilating data from a simulated global constellation of stratospheric balloons. *Quarterly Journal of the Royal Meteorological Society*, 130(602):2475–2493, 2004.

[18] Todd McKinney, Nick Perlaky, Evan Danielson, Areeb Mohammed, Jackson Lee, Ben O'Bryan, Connor Stoll, Clara Hochmuth, Tyler Gallien, Skyler Kerr, et al. Around the world they go: Circumnavigating balloon satellites! *Bulletin of the American Meteorological Society*, 104(1):E192–E207, 2023.

[19] Todd McKinney, Nick Perlaky, Mike Newchurch, and Bill Brown. Insights on polar day antarctica radio propagation using amateur radio beacons on circumnavigating balloons. *Atmosphere*, 14(7):1118, 2023.

[20] NIBBB. Northern illinois bottlecap balloon brigade, 2023. Accessed 5 February 2023, url = https://nibbb.org/.

[21] G Dwayne Orr, Andrew S Denny, and Jill Juneau. Csbf engineering overview and new iridium capabilities for ldb. In *AIAA Balloon Systems (BAL) Conference*, page 1374, 2013.

[22] Florence Rabier, Aurélie Bouchard, Eric Brun, Alexis Doerenbecher, Stéphanie Guedj, Vincent Guidard, Fatima Karbou, Vincent-Henri Peuch, Laaziz El Amraoui, Dominique Puech, et al. The concordiasi project in antarctica. *Bulletin of the American Meteorological Society*, 91(1):69–86, 2010.

[23] Mathieu Ratynski, Sergey Khaykin, Alain Hauchecorne, Robin Wing, Jean-Pierre Cammas, Yann Hello, and Philippe Keckhut. Validation of aeolus wind profiles using ground-based lidar and radiosonde observations at réunion island and the observatoire de haute-provence. *Atmospheric Measurement Techniques*, 16(4):997–1016, 2023.

[24] RZ Sagdeev, VM Linkin, VV Kerzhanovich, AN Lipatov, AA Shurupov, JE Blamont, D Crisp, AP Ingersoll, LS Elson, RA Preston, et al. Overview of vega venus balloon in situ meteorological measurements. *Science*, 231(4744):1411–1414, 1986.

[25] MS Smith and EL Rainwater. Optimum designs for superpressure balloons. *Advances in Space Research*, 33(10):1688–1693, 2004.

[26] AF Stein, Roland R Draxler, Glenn D Rolph, Barbara JB Stunder, MD Cohen, and Fong Ngan. Noaa's hysplit atmospheric transport and dispersion modeling system. *Bulletin of the American Meteorological Society*, 96(12):2059–2077, 2015.

[27] Ad Stoffelen, GJ Marseille, F Bouttier, D Vasiljevic, S De Haan, and C Cardinali. Adm-aeolus doppler wind lidar observing system simulation experiment. *Quarterly Journal of the Royal Meteorological Society: A journal of the atmospheric sciences, applied meteorology and physical oceanography*, 132(619):1927–1947, 2006.

[28] DW Tarasick, TK Carey-Smith, WK Hocking, O Moeini, H He, J Liu, MK Osman, AM Thompson, BJ Johnson, SJ Oltmans, et al. Quantifying stratosphere-troposphere transport of ozone using balloon-borne ozonesondes, radar windprofilers and trajectory models. *Atmospheric Environment*, 198:496–509, 2019.

[29] J. Taylor. Weak signal propogation reporter network (WSPRnet), 2022. Accessed 5 May 2022, https://wsprnet.org/drupal/.

[30] Andre Vargas. Overview of the french balloon program for the 2011-2012 period. In *AIAA Balloon Systems (BAL) Conference*, page 1314, 2013.

[31] W5KUB. Amateur radio roundtable, 2023. Accessed 5 February 2023, url = https://tmedlin.com/.

[32] Christine Wesche, Rolf Weller, Gert König-Langlo, Tanja Fromm, Alfons Eckstaller, Uwe Nixdorf, and Eberhard Kohlberg. Neumayer iii and kohnen station in antarctica operated by the alfred wegener institute. *Journal of large-scale research facilities JLSRF*, 2:A85–A85, 2016.

[33] Nobuyuki Yajima, Naoki Izutsu, Hideyuki Honda, Haruhisa Kurokawa, and Kiyoho Matsushima. Three-dimensional gore design concept for high-pressure balloons. *Journal of aircraft*, 38(4):738–744, 2001.

[34] YokohamaBalloons. Sphere balloon(32inch), 2023. Accessed 5 February 2023, url = https://yokohamaballoon.com/products/sphere-balloon32inch?variant=41763086729369.

[35] Yi Zhang and Dongxu Liu. Influences of initial launch conditions on flight performance of high altitude balloon ascending process. *Advances in Space Research*, 56(4):605–618, 2015.